A facile method to fabricate AC/CuO for efficient removal of organic pollutants by adsorption and persulfate-based advanced oxidation processes

Youlin Li, Yu Hu, Wenqiao You, Guangming Zhou and Guilong Peng

ABSTRACT

Activated carbon/CuO (AC/CuO) composites were prepared through a facile one-step hydrothermal method and used as a bifunctional material for adsorption and catalysis degradation of bisphenol A (BPA). The composite was characterized by Fourier transform infrared spectroscopy (FT-IR), scanning electron microscopy (SEM), and X-ray powder diffraction (XRD). The obtained AC/CuO exhibited excellent adsorption and catalytic performance. The maximum adsorption capacity of BPA on the AC/CuO was 319.03 mg/g according to the Langmuir fitting. At an initial BPA concentration of 20 mg/L, the BPA degradation efficiencies were maintained above 96% for 15 min by using 20 mg/L AC/CuO and 2 mM peroxymonosulfate (PMS). Moreover, the relationship between adsorption and catalytic degradation was also investigated. The results indicated that the pre-adsorption disfavored the degradation reaction. This work not only provides a novel preparation method for AC/CuO catalyst, but also gives a deeper insight into the mechanisms between adsorption and catalytic degradation.

Key words | activated carbon/CuO, adsorption, bisphenol A, degradation, peroxymonosulfate

Youlin Li
Yu Hu
Wenqiao You
Guangming Zhou (corresponding author)
Guilong Peng
Key Laboratory of Luminescence and Real-Time Analytical Chemistry (Southwest University), Ministry of Education, School of Chemistry and Chemical Engineering,
Southwest University,
Chongqing 400715,
China
E-mail: *847109380@qq.com*

Guilong Peng
State Key Laboratory of Silkworm Genome Biology, Key Laboratory of Sericultural Biology and Genetic Breeding, Ministry of Agriculture and Rural Affairs, College of Sericulture, Textile and Biomass Sciences,
Southwest University,
Chongqing 400715,
China

HIGHLIGHTS

- Activated carbon/CuO (AC/CuO) was prepared through a facile one-step hydrothermal method.
- The obtained AC/CuO exhibited excellent adsorption and catalytic performance.
- The relationship between adsorption and catalytic degradation was thoroughly investigated.

INTRODUCTION

In recent years, with the introduction of new chemicals into the environment, the pollution of refractory organics to the environment has become a challenging multidisciplinary problem. Various techniques, such as advanced oxidation (Xi *et al.* 2014), adsorption (Bautista-Toledo *et al.* 2014), membrane separation (Yüksel *et al.* 2013) and biological treatment (Urase & Kikuta 2005), have been developed for the removal of organic pollutants from aqueous solution. Currently, the adsorption process is still recognized as one of the most commonly used methods to treat wastewater containing organic compounds due to its low cost, effectiveness and environmental friendliness (Zhang *et al.* 2010; Zhou *et al.* 2020), but the pollutants cannot be decomposed to small molecule compounds or completely eliminated. In recent years, an advanced oxidation process (AOPs) based on persulfate (PS) has been successfully applied to the degradation and mineralization of organic pollutants (Wang *et al.* 2019; Yang *et al.* 2020). In this process, sulfate radical ($SO_4^{\bullet -}$) and hydroxyl radical (•OH) with high redox potential of 2.5–3.1 and 2.8 eV, respectively, can be generated by activation of PS (Pang *et al.* 2019). PS includes peroxydisulfate (PDS) and peroxymonosulfate (PMS). Compared with PDS, PMS is

doi: 10.2166/aqua.2020.094

more easily activated due to its shorter bond length of O-O (Rastogi *et al.* 2009).

The combination of adsorption process and AOPs can further guarantee the high removal of organic pollutants. Therefore, it is of great significance to seek novel materials with high adsorption capacity, fast adsorption rate, and high catalytic activity for the oxidative degradation of pollutants. In addition, enriching organic pollutants from aqueous solutions to the surface of the catalysts is considered an effective strategy because, in most cases, oxidative free radicals are generated on the surface of the catalyst (Lee *et al.* 2013). For example, activated carbon (AC) and biochar were reported as supports for metal oxides in PS activation for organic pollutants degradation (Muhammad *et al.* 2012; Jonidi Jafari *et al.* 2017; Li *et al.* 2020a, 2020b), and these results showed the high adsorption capacity of the catalysts could promote the reaction of pollutants with oxidative species. The above promotion effect was attributed to the enrichment of pollutants on the catalyst surface through adsorption.

Wang *et al.* (2017) reported a novel strategy for the removal of refractory organic contaminants through a sludge-derived biochar (SDBC)/PS system via both an adsorption and advanced oxidation process under ambient conditions. The results show that the degradation efficiency of AOPs can be promoted by combining the adsorption and activation of PS in a heterogeneous catalyst system. Peng *et al.* (2019) studied the removal of enrofloxacin by magnetic montmorillonite via adsorption and persulfate oxidation and found that the degradation efficiency decreased significantly with the increase of pre-adsorption time. However, the relationship between adsorption and catalytic degradation was not investigated in detail in these reports.

In this study, considering the good adsorption performance of AC and the high catalytic activity of CuO (Hu *et al.* 2017), AC/CuO composites were synthesized under mild hydrothermal conditions with low cost and used as adsorption-catalysis bifunctional material. This material can preconcentrate organic pollutants on its surface, and then catalytically activate specific oxidants to generate reactive oxygen species (ROS) for the *in situ* degradation of the adsorbed pollutants (Chen *et al.* 2020). In order to deeply explore the relationship between adsorption and degradation, bisphenol A (a typical endocrine disruptor) was selected as the model contaminant for removal. A new insight of the mechanisms between adsorption and catalytic degradation was proposed.

MATERIALS AND METHODS

Reagents

PMS ($2KHSO_5{\cdot}KHSO_4{\cdot}K_2SO_4$ as oxone) and bisphenol A (BPA) were purchased from Sigma-Aldrich (St. Louis, MO, USA). Activated carbon (AC), cupric nitrate ($Cu(NO_3)_2{\cdot}3H_2O$), ammonia ($NH_3{\cdot}H_2O$), sodium hydroxide (NaOH), sulfuric acid (H_2SO_4), sodium chloride (NaCl), sodium bicarbonate ($NaHCO_3$), methanol (MeOH), ethanol (EtOH), tert-butyl alcohol (TBA), sodium humic acid (HA) and other chemical reagents were purchased from Sinopharm Chemical Reagent Co., Ltd, (Shanghai, China). All chemicals were of at least analytical grade and were used as received without further purification. A basic FE28 pH meter (Mettler Toledo, Shanghai, China) was used to measure the pH values. Ultrapure water from a Milli-Q academic water purification system was used to prepare all the solutions required in the present work.

Preparation of AC/CuO

The AC/CuO composite was fabricated using a modified simple and one-step hydrothermal method according to the reported method (Li *et al.* 2019). $Cu(NO_3)_2{\cdot}3H_2O$ (5.0 g) and AC were mixed with different mass ratios of 2:1, 1:1, 1:1.5, and 1:2 (i.e. the dosage of AC was 2.5, 5, 7.5 and 10 g, respectively) in ultrapure water, the mixed solution was mechanically stirred for 5 min at room temperature. After that, 5 mL $NH_3{\cdot}H_2O$ was added into the above-mixed solution until the pH reached about 10, thereafter, a blue suspension was generated. The reaction was conducted at 80 °C for 6 h and the air was continuously purged into the mixture with a peristaltic pump. The resulting precipitate was separated by filtration and washed with ultrapure water. Finally, the obtained AC/CuO was collected and dried at 105 °C. The formation reactions of CuO nanoparticles can be expressed as Equations (1) and

(2). For a comparison, CuO nanoparticles were prepared in a similar procedure without adding activated carbon:

$$Cu(NO_3)_2 + 2NH_3 \bullet H_2O \rightarrow Cu(OH)_2 + 2NH_4NO_3 \quad (1)$$

$$Cu(OH)_2 \rightarrow CuO + H_2O \quad (2)$$

Experimental procedures

The adsorption experiments were carried in a 150 mL conical flask at 25 °C under shaking (150 rpm). The adsorption behaviors of the AC/CuO were quantified in terms of adsorption kinetics, adsorption isotherm and pH effect experiments with 100 mL of BPA solution. In adsorption kinetic experiments, the initial concentration of the AC/CuO was fixed at 20 mg/L (pH 6.0). The adsorption isotherm experiments were conducted with initial concentrations of BPA in the range of 10–50 mg/L. In the pH effect experiments, the initial solution pH ranged from 3.52 to 11.08 without adjusting during the adsorption process.

The experiments to evaluate the degradation of BPA in solution by activating PMS with AC/CuO were conducted in the same conical flasks as used in the adsorption experiments, and 20 mg/L of AC/CuO was dispersed into 100 mL BPA (20 mg/L) solution. Subsequently, aliquots of a PMS stock solution were spiked into the reactors at a concentration of 2.0 mM to start the degradation reaction. At fixed time intervals, 1 mL of sample was withdrawn and immediately quenched with methanol and filtered through a 0.22-μm membrane for further analysis by high performance liquid chromatography (HPLC). All experiments were repeated in triplicate.

Analytical methods

For the adsorption experiments, the concentrations of BPA were measured by a UV-vis spectrophotometer (UV-1900, Shimadzu, Japan) at a wavelength of 275 nm. For the degradation experiments, the concentrations of BPA were analyzed on an HPLC system (Shimadzu, Kyoto, Japan) equipped with two pumps LC-20AT, SPD-20A, UV-Vis detector and a LC solution work-station. A Phenomenex C18 (5 μm, 150 × 4.6 mm) was used for the separation of organic compounds at 35 °C. The mobile phase consisted of methanol (85%) and 0.2% acetic acid in water (15%), at a flow rate of 1.0 mL/min, and the injection volume was 20 μL.

RESULTS AND DISCUSSION

Optimization of the dosage of AC

The adsorbed amounts (q_e) of BPA on the CuO, AC as well as the AC/CuO obtained with different amounts of AC are shown in Figure 1. CuO exhibited the low adsorbed amount of 11.16 mg/g and the adsorption amount of BPA increased substantially with the increase of AC-loaded amount, indicating that AC was the key component for BPA adsorption. The AC/CuO prepared with the addition of 7.5 g AC had a similar adsorption amount of BPA with AC, but with the addition of 10.0 g AC had a slightly lower adsorption amount of BPA than that of 7.5 g AC. Thus, the addition of 7.5 g AC was selected to prepare AC/CuO composite in the subsequent experiments.

Characterizations of prepared AC/CuO

In order to investigate the morphology of obtained materials, a comparison between SEM images of the raw

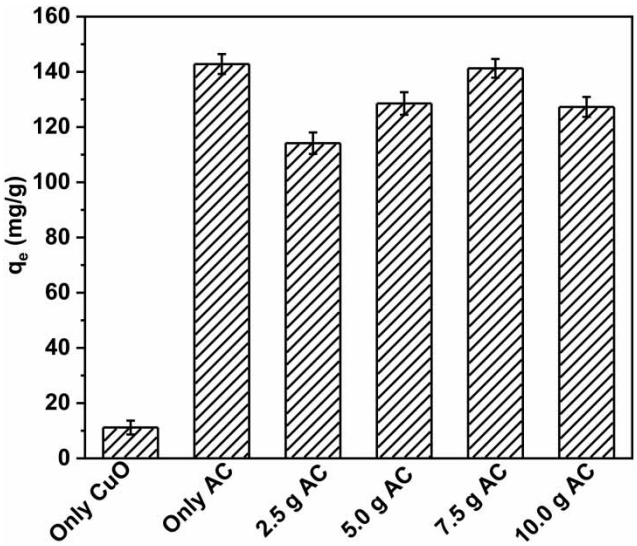

Figure 1 | Adsorption of BPA on the CuO, AC as well as the AC/CuO obtained with different amounts of AC.

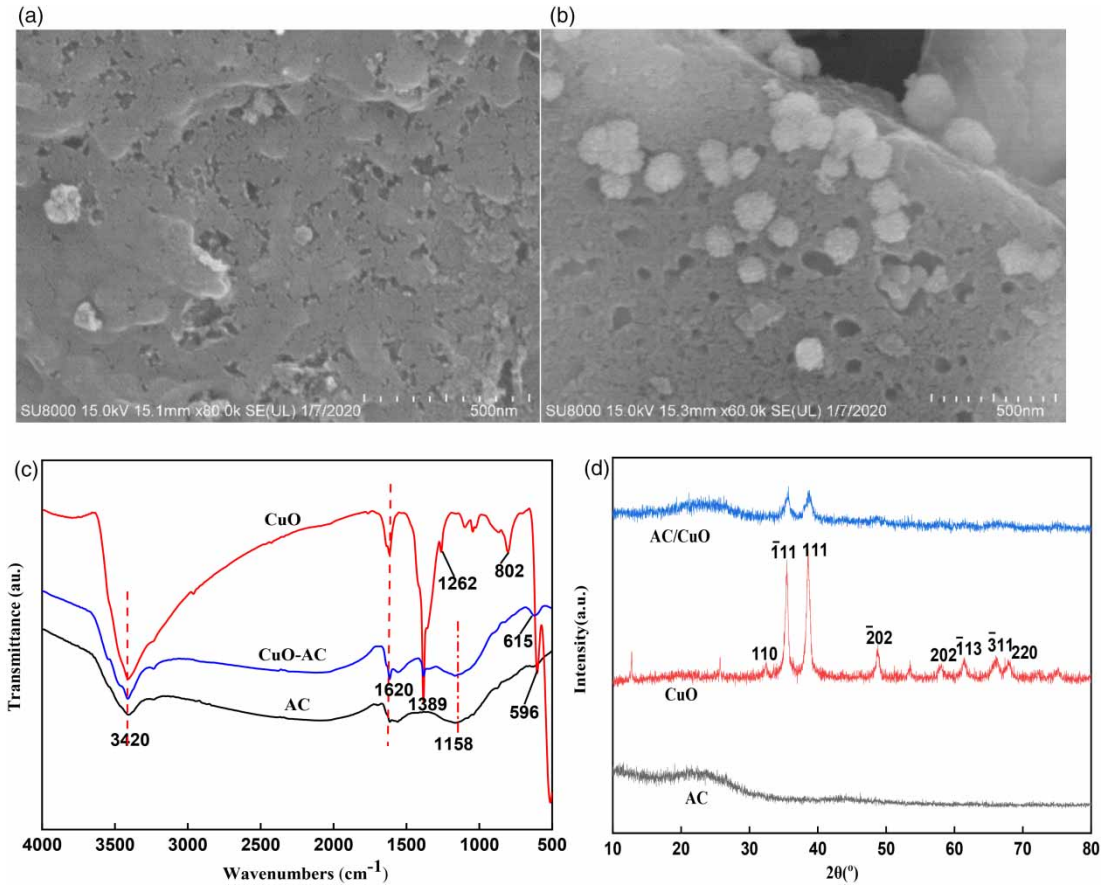

Figure 2 | SEM images of raw AC (a) and AC/CuO (b) as well as FTIR spectra (c) and XRD patterns of AC, CuO, AC/CuO (d).

AC and AC/CuO is shown in Figure 2. The AC has some pore structure (Figure 2(a)) and the surface of the AC/CuO has many spherical particles (Figure 2(b)). The CuO particles with an average size of 50–100 nm were adhered on the surface of AC, also, some particles were embedded into the pores of AC, which proved the surface of AC/CuO has already generated the corresponding composites. The specific surface areas and pore characteristics of the AC and AC/CuO are summarized in Table S1. The average diameters of AC/CuO are larger than those of the original PAC, and the specific surface area for AC and AC/CuO area is 920 and 731 m^2/g, respectively, and total pore volume is reduced (Table S1).

The FTIR spectra of AC, CuO, and AC/CuO are shown in Figure 2(c). The typical broad peak from 3,200 to 3,670 cm^{-1} could be attributed to the O–H stretching vibration, which was from the H_2O molecules and hydroxyl compounds in the samples (Hu *et al.* 2016). The band at 1,620 cm^{-1} was assigned to the stretching vibration of residual C = O (Li *et al.* 2020b). The bands at 596 and 802 cm^{-1} of CuO spectrum could be attributed to Cu-O vibration, indicating the existence of CuO (Gholami *et al.* 2020). Compared to AC/CuO, the shift of peaks at 596–615 cm^{-1} implied the interaction between CuO and AC. Note that the bands of CuO at 1,262 and 1,389 cm^{-1} disappeared and a new broad band appeared at 1,158 cm^{-1} in the FTIR spectra of AC/CuO which could be ascribed to the formation of a Cu-O-C bond (Du *et al.* 2019).

The X-ray diffraction (XRD) spectra of AC, AC/CuO and CuO are represented in Figure 2(d). The broad diffraction peak at $2\theta = 23°$ was assigned to the characteristic reflection of amorphous carbon (Jonidi Jafari *et al.* 2017). The XRD pattern of CuO presented seven diffraction peaks at 2θ angles of 35.4, 38.5, 48.9, 58.1, 61.5 and 66.1°,

which matched well with the (111), (111), (202), (202), (113) and (311) planes of the tetragonal CuO spinel (JCPDS File No. 80-1916) (Chang *et al.* 2018). Moreover, in the XRD pattern of AC/CuO, only two obvious diffraction peaks, i.e. ($^{-}$111) and (111), could be observed, which may be attributed to the low CuO concentration in the sample, beyond the detection limit of the equipment.

Adsorption kinetics and adsorption isotherms

The adsorption kinetics of BPA on the AC/CuO are presented in Figure 3(a), and the pseudo-second-order model was used to fit the kinetic data. The results indicated that due to the large number of adsorption sites on the surface of the AC/CuO in the early stage, the adsorption increased rapidly in the first 60 min and the adsorption rate rapidly reduced and gradually reached equilibrium; this could be attributed to the site being occupied and the adsorption rate decrease. When the adsorption time is 150–300 min, it tends to be stable. Based on the above results, in subsequent adsorption experiments, we believed that the adsorption equilibrium was achieved at 150 min. Kinetic parameters obtained from the pseudo-second-order model are listed in Table S2. The initial adsorption rate (v_0) of BPA was 19.96 mg/g/min and the equilibrium adsorbed amount (q_e) was 97.29 mg/g, with an R^2 of 0.9751. The obtained results were in good agreement with the experimental values. Therefore, in the present study, a pseudo-second-order model was suitable for describing the adsorption kinetics process of BPA on AC/CuO. This may indicate that in addition to the adsorption onto the surface sites, the adsorption process also involves mass transfer and intra-particle diffusion (Annadurai *et al.* 2008). In other words, during the BPA adsorption process, after the BPA molecules are initially adsorbed onto the AC/CuO surface controlled by molecular diffusion, they enter the internal pore structure of AC/CuO under the action of intra-particle diffusion, are gradually adsorbed by the interior surface of AC/CuO and finally reach the adsorption equilibrium.

Adsorption isotherms are used to describe the process of dynamic equilibrium between adsorbent and adsorbate. Langmuir and Freundlich isotherm models are used to fit the adsorption equilibrium data to study the adsorption mechanism (Qiao *et al.* 2020). Based on the experimental data, the adsorption isotherms of BPA on the AC/CuO were plotted (Figure 3(b)), and the fitting results are presented in Table S3. As for the Langmuir model, according to the fitting results, the maximum adsorption capacity (q_m) for BPA was 319.03 mg/g, and the high adsorption capacity could be attributed to its high specific surface (731 m^2/g). Furthermore, a highly linear relationship ($R^2 = 0.9993$) was acquired, which assumed the adsorption of BPA on the AC/CuO was mainly in the form of monolayer coverage, indicating that chemical adsorption may play an important role for BPA adsorption on AC/CuO. Based on the Freundlich model, which was suitable for multi-layer adsorption on a non-uniform surface, a good

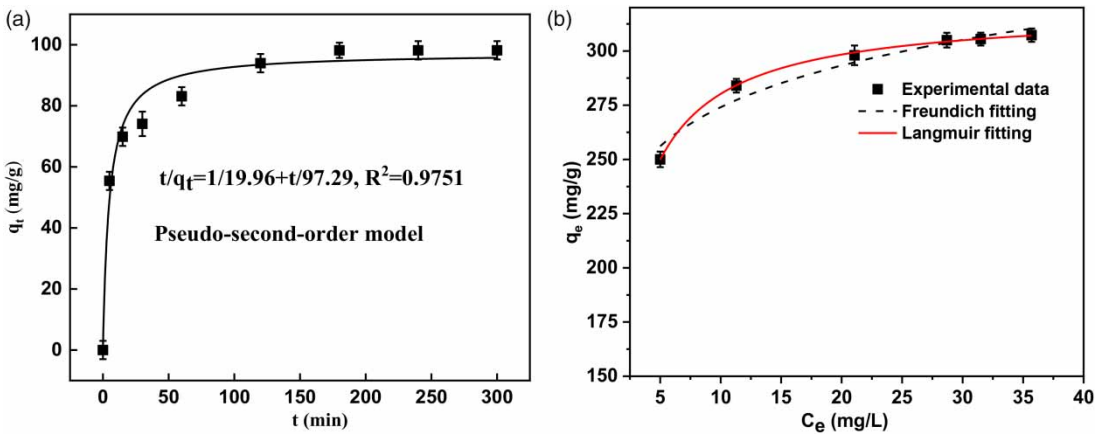

Figure 3 | Adsorption kinetics of BPA on AC/CuO (a); and adsorption isotherms of BPA on AC/CuO (b).

linear relationship ($R^2 = 0.9556$) was obtained, demonstrating that the adsorption of BPA by AC/CuO may also be closely related to physical interaction. The values of the heterogeneity factor $1/n$ was less than 1, indicating that the adsorption is facile and favorable (Tang *et al.* 2018). Considering the good linear relationship of these two typical models, it could be concluded that both chemical and physical interactions were significant for BPA adsorption by AC/CuO.

Effect of pH on the adsorption

The pH value of the solution has an important influence on the absorption of BPA, since it determines the surface charge of the adsorbent and the speciation of the adsorbate. From Figure 4(a), it can be seen that the BPA adsorption capacity was constant in a pH range of 3.52–9.25, while a much higher BPA uptake was observed when the pH was 11.08. BPA is a neutral molecule and speciates into divalent anions at pH > 9.6 (Figure 4(b)) (Lin *et al.* 2012), and the surface of the AC/CuO was positively charged in the pH ranges of 3.01–11.02 (Figure S1). Electrostatic attraction interaction promoting the adsorption can occur between the negatively charged BPA molecules and positively charged AC/CuO surface, leading to the high adsorption capacity for BPA at pH of 11.02, while hydrophobic interaction and hydrogen bonds should be dominant for the adsorption of BPA on AC/CuO at low pH (pH < 9) conditions.

Catalytic degradation of BPA

The AC/CuO was further applied as catalyst for the catalyzed PMS oxidative degradation of BPA. As can be seen from Figure 5(a), only a small amount of BPA removal (<5%) was achieved by PMS or CuO alone within 15 min, suggesting that PMS could barely oxidize BPA, and CuO showed no adsorption of BPA. So, PMS could not efficiently degrade BPA, and the adsorption of BPA by CuO was negligible. The removal of BPA in the presence of AC and AC/CuO alone was approximately 32 and 28%, respectively. The degradation of BPA by a combination of AC and PMS increased slightly but was still less than 42%, implying that the activity of AC in the presence of PMS was very weak with the rate constants (k_{obs}) of $3.16 \times 10^{-2}\,min^{-1}$. It is worth noting that the functional groups such as –C–OH and –COOH on the surface of AC/CuO can directly activate PMS to produce $^1O_2$ (Li *et al.* 2020b). However, when the AC/CuO and PMS were used together, more than 96% of BPA was degraded within 15 min, which was much higher than that of the CuO/PMS system (54%). Therefore, AC/CuO showed excellent adsorptive and catalytic performances for the degradation of BPA in the presence of PMS. Figure 5(b) shows HPLC chromatograms for BPA degradation in the AC/CuO/PMS system, revealing that the peak area at a retention time of ~3.8 min gradually decreased with the extension of the reaction time, indicating the fast degradation of BPA. Thus, the catalytic ability of the AC/CuO was much greater than that of AC and CuO. Based

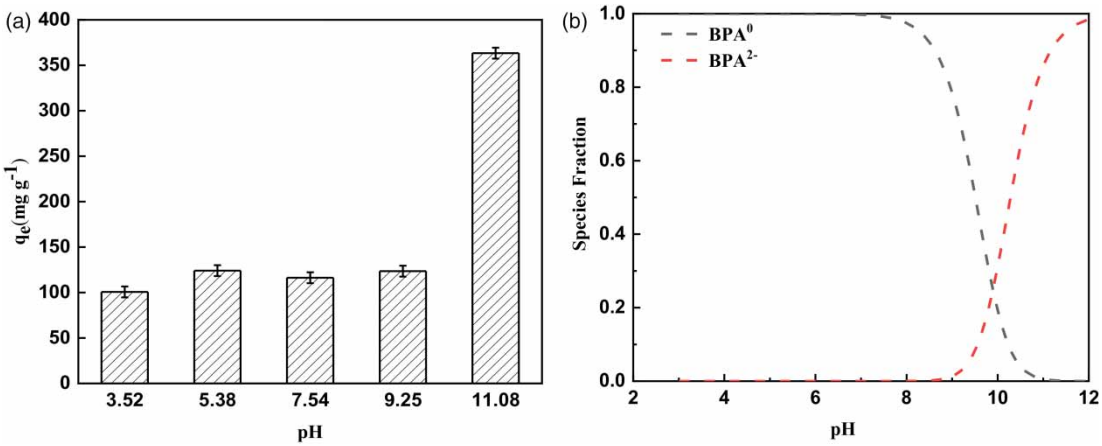

Figure 4 | The effect of pH on the adsorption properties of BPA by AC/CuO adsorbent (a) and BPA speciation calculated based on BPA pKa values (b).

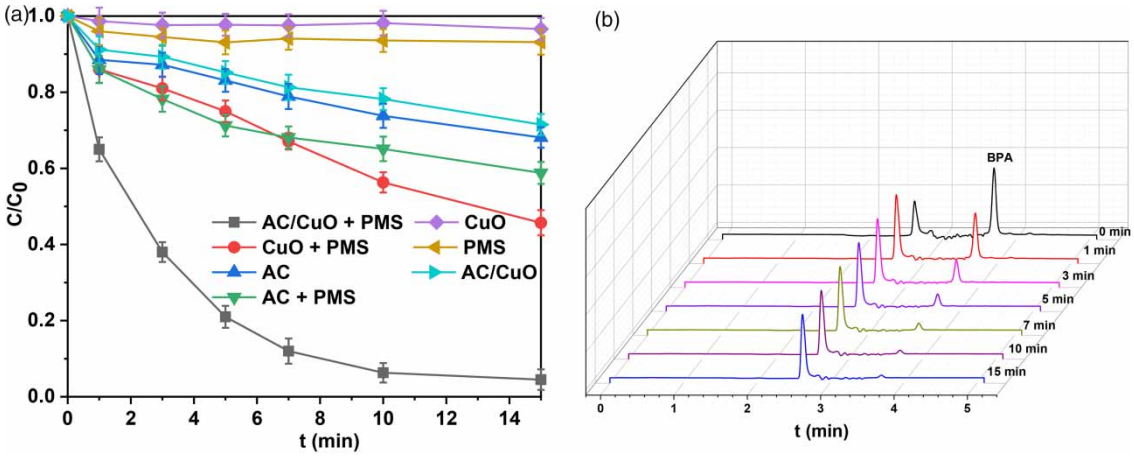

Figure 5 | Removal efficiencies of BPA in different systems (a) and HPLC chromatograms recorded at various reaction times for BPA degradation in the AC/CuO/PMS system (b).

on the above adsorption and degradation experiment results, it can be fully confirmed that AC and CuO show a good synergy in the activation of PMS to degrade BPA. This high performance could be ascribed to the fact that both adsorption and oxidation were involved in the removal of BPA simultaneously. Thus, it can be concluded that AC has adsorption performance, whereas CuO offers catalytic ability, and the excellent performance of AC/CuO in the presence of PMS to remove BPA was attributed to its adsorption ability and catalytic performance of the AC/CuO.

Possible mechanism for BPA degradation

In general, $SO_4^{\bullet-}$ and •OH are the potential ROS for pollutants removal in PMS-based AOPs (Ding *et al.* 2013). Hence two commonly used quenchers, ethanol (EtOH) and tert-butanol (TBA), were used as free radical scavengers to verify the formation of $SO_4^{\bullet-}$ and •OH. EtOH can quench both •OH ($k_{\cdot OH} = 1.9 \times 10^9\ M^{-1}\ s^{-1}$) and $SO_4^{\bullet-}$ ($k_{SO_4^{\bullet-}} = 1.6 \times 10^7\ M^{-1}\ s^{-1}$), and TBA is considered as a powerful •OH scavenger ($k_{\cdot OH} = 6.0 \times 10^8\ M^{-1}\ s^{-1}$) but poor reactivity with $SO_4^{\bullet-}$ ($k_{SO_4^{\bullet-}} = 4.0 \times 10^5\ M^{-1}\ s^{-1}$) (Huang *et al.* 2017). As depicted in Figure S2, more than 96% of BPA could be removed in the control experiment. However, BPA degradation efficiencies were inhibited in the presence of different concentrations of TBA or EtOH into the reaction system, indicating that $SO_4^{\bullet-}$ and •OH were indeed the dominant ROS. The addition of 10 and 100 mM EtOH resulted in decreasing BPA removal (in 15 min) to 52 and 29%, respectively. Meanwhile, as the concentrations of TBA increased to 10 and 100 mM, the degradation efficiency of BPA decreased from 96% to 65 and 46%, respectively. It is fully confirmed that the inhibition was enhanced with the increasing scavenger dosage, which may be due to the scavenging of TBA with both the $SO_4^{\bullet-}$ and •OH other than the •OH alone. The quenching ability of TBA was obviously weaker than that of MeOH, indicating that $SO_4^{\bullet-}$ should be recognized as the dominant ROS, and •OH was also involved for the oxidative degradation in the AC/CuO/PMS process. Based on all the above results and previous reports (Ding *et al.* 2013; Li *et al.* 2020b), the mechanism of activation of PMS by AC/CuO was proposed as follows:

$$\text{AC-surface-COOH} + HSO_5^- \rightarrow \text{AC-surface-OO}^{\bullet-} + SO_4^{2-} + 1/2^1O_2 + 2H^+ \quad (3)$$

$$\text{AC-surface-OH} + HSO_5^- \rightarrow \text{AC-surface-O}^{\bullet-} + SO_4^{2-} + 1/2^1O_2 + 2H^+ \quad (4)$$

$$Cu^{2+} + HSO_5^- \rightarrow Cu^+ + SO_5^{\bullet-} + H^+ \quad (5)$$

$$Cu^+ + HSO_5^- \rightarrow Cu^{2+} + SO_4^{\bullet-} + OH^- \quad (6)$$

$$SO_4^{\bullet-} + H_2O \rightarrow \bullet OH + H^+ + SO_4^{2-} \quad (7)$$

Relationship between adsorption and catalytic degradation

Wang *et al.* (2015) prepared nitrogen-doped reduced graphene oxide (N-RGO), used as a bifunctional material for removing bisphenols (BPs) via adsorption and degradation. Their research results show that BPs contaminants that have been adsorbed onto the material could be degraded by persulfate oxidation, leading to a further increase in the adsorption of the residual BPs. However, many researchers pointed out that once the pollutants have been adsorbed on the material surface, they can barely be removed in the presence of PS (Liang *et al.* 2009; Yang *et al.* 2011; Peng *et al.* 2019). To further investigate the influence of adsorption and catalytic degradation, comparative degradation kinetics experiments were performed by changing the pre-adsorption time. As shown in Figure 6(a), it is apparent that the BPA degradation efficiency decreased with the extension of the pre-adsorption time. With the pre-adsorption time increased from 0 to 30 min, the k_{obs} values for BPA degradation decreased from 2.13×10^{-1} to 3.21×10^{-2} min^{-1}. This phenomenon could be attributed to the fact that more and more adsorptive active sites were occupied due to the adsorbed BPA on the AC/CuO surface increase, and the adsorption sites also acted as catalytic active sites, leading to the degradation rates decrease (Xiao *et al.* 2018). Therefore, pre-adsorption of pollutants was not conducive for further degradation, which was due to competition of the active sites between adsorption and catalytic activation (Zhang *et al.* 2019). In order to better explain the great influence of pre-adsorption on degradation, the AC/CuO after degradation was eluted with MeOH and analyzed by HPLC. As can be seen from Figure 6(b), almost no BPA could be detected on the used AC/CuO without pre-adsorption before PMS was added into the reaction solution to start the degradation reaction, and the residual amount of BPA on the used AC/CuO increased with the increase of pre-adsorption time. Interestingly, the used pre-adsorption 30 min AC/CuO and the only adsorption 30 min AC/CuO have almost the same residual amount of BPA, which further confirmed that once the pollutants have been adsorbed on the material surface, they are difficult to remove by degradation. Without pre-adsorption, during the process of synchronous adsorption and catalytic degradation, the removal of pollutants is degraded rather than adsorbed on the material. Thus, the synergistic effect between adsorption and catalytic degradation promoted the effective removal of pollutants.

CONCLUSIONS

In summary, a facile and economical approach under mild hydrothermal conditions for the synthesis of AC/CuO composites was established. The obtained AC/CuO had high adsorption capacities for BPA (319.03 mg/g) and it also exhibited superior catalytic performance for PMS activation for BPA removal. The high-efficiency adsorption

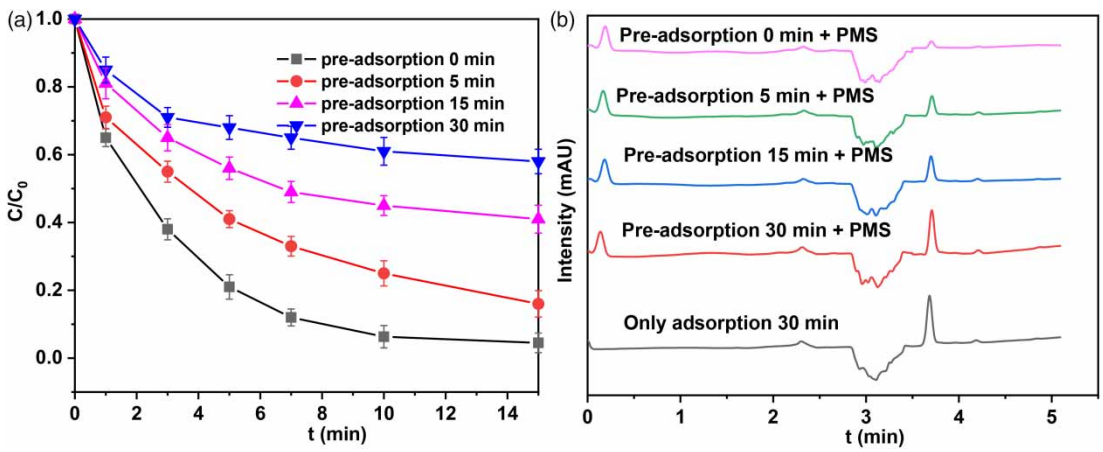

Figure 6 | Effect of the pre-adsorption time on degradation (a) HPLC chromatograms of ENR residue on the AC/CuO (b).

performance of the AC/CuO greatly promoted the catalytic efficiency. Thus, 96% of BPA (20 mg/L) could be removed within 15 min at a PMS dose of 2 mM in the presence of 20 mg/L AC/CuO. In addition, the relationship between adsorption and catalytic degradation was further elucidated. We further confirmed that the pre-adsorption of pollutants was not conducive for further catalytic degradation, once the pollutants have been adsorbed on the material surface, they could barely be removed via catalytic degradation due to many active sites that were occupied by the pollutants adsorbed on the surface. This work provided a new insight in understanding the synergistic effect between catalytic degradation and adsorption.

ACKNOWLEDGEMENTS

This study was supported by the financial support from the Central Universities (SWU119058), the National Nature Science Foundation of China (Project no. 51779020), and the Natural Scientific Fund of Chongqing (No. cstc2020jcyj-msxm1625).

DATA AVAILABILITY STATEMENT

All relevant data are included in the paper or its Supplementary Information.

REFERENCES

Annadurai, G., Ling, L. Y. & Lee, J.-F. 2008 Adsorption of reactive dye from an aqueous solution by chitosan: isotherm, kinetic and thermodynamic analysis. *Journal of Hazardous Materials* **152**, 337–346.

Bautista-Toledo, M. I., Rivera-Utrilla, J., Ocampo-Pérez, R., Carrasco-Marín, F. & Sánchez-Polo, M. 2014 Cooperative adsorption of bisphenol-A and chromium(III) ions from water on activated carbons prepared from olive-mill waste. *Carbon* **73**, 338–350.

Chang, B., Hao, S., Ye, Z. & Yang, Y. 2018 A self-supported amorphous Ni–P alloy on a CuO nanowire array: an efficient 3D electrode catalyst for water splitting in alkaline media. *Chemical Communications* **54**, 2393–2396.

Chen, M., Wang, N. & Zhu, L. 2020 Single-atom dispersed Co-N-C: a novel adsorption-catalysis bifunctional material for rapid removing bisphenol A. *Catalysis Today* **348**, 187–193.

Ding, Y., Zhu, L., Wang, N. & Tang, H. 2013 Sulfate radicals induced degradation of tetrabromobisphenol A with nanoscaled magnetic $CuFe_2O_4$ as a heterogeneous catalyst of peroxymonosulfate. *Applied Catalysis B: Environmental* **129**, 153–162.

Du, X., Zhang, Y., Si, F., Yao, C., Du, M., Hussain, I., Kim, H., Huang, S., Lin, Z. & Hayat, W. 2019 Persulfate non-radical activation by nano-CuO for efficient removal of chlorinated organic compounds: reduced graphene oxide-assisted and CuO (0 0 1) facet-dependent. *Chemical Engineering Journal* **356**, 178–189.

Gholami, P., Dinpazhoh, L., Khataee, A., Hassani, A. & Bhatnagar, A. 2020 Facile hydrothermal synthesis of novel Fe-Cu layered double hydroxide/biochar nanocomposite with enhanced sonocatalytic activity for degradation of cefazolin sodium. *Journal of Hazardous Materials* **381**, 120742–120757.

Hu, Z.-P., Zhu, Y.-P., Gao, Z.-M., Wang, G., Liu, Y., Liu, X. & Yuan, Z.-Y. 2016 Cuo catalysts supported on activated red mud for efficient catalytic carbon monoxide oxidation. *Chemical Engineering Journal* **302**, 23–32.

Hu, J., Dong, H., Qu, J. & Qiang, Z. 2017 Enhanced degradation of iopamidol by peroxymonosulfate catalyzed by two pipe corrosion products (CuO and δ-MnO2). *Water Research* **112**, 1–8.

Huang, G.-X., Wang, C.-Y., Yang, C.-W., Guo, P.-C. & Yu, H.-Q. 2017 Degradation of bisphenol A by peroxymonosulfate catalytically activated with Mn1.8Fe1.2O4 nanospheres: synergism between Mn and Fe. *Environmental Science & Technology* **51**, 12611–12618.

Jonidi Jafari, A., Kakavandi, B., Jaafarzadeh, N., Rezaei Kalantary, R., Ahmadi, M. & Akbar Babaei, A. 2017 Fenton-like catalytic oxidation of tetracycline by AC@Fe3O4 as a heterogeneous persulfate activator: adsorption and degradation studies. *Journal of Industrial and Engineering Chemistry* **45**, 323–333.

Lee, Y.-C., Lo, S.-L., Kuo, J. & Huang, C.-P. 2013 Promoted degradation of perfluorooctanic acid by persulfate when adding activated carbon. *Journal of Hazardous Materials* **261**, 463–469.

Li, G., Zhong, Z. H., Yang, C., He, Q. & Peng, G. L. 2019 Degradation of Acid Orange 7 by peroxymonosulfate activated by cupric oxide. *Journal of Water Supply Research and Technology – Aqua* **68**, 29–38.

Li, W., Liu, B., Wang, Z., Wang, K., Lan, Y. & Zhou, L. 2020a Efficient activation of peroxydisulfate (PDS) by rice straw biochar modified by copper oxide (RSBC-CuO) for the degradation of phenacetin (PNT). *Chemical Engineering Journal* **395**, 125094–125105.

Li, Z., Liu, D., Huang, W., Wei, X. & Huang, W. 2020b Biochar supported CuO composites used as an efficient peroxymonosulfate activator for highly saline organic wastewater treatment. *Science of the Total Environment* **721**, 137764–137775.

Liang, C., Lin, Y.-T. & Shih, W.-H. 2009 Treatment of trichloroethylene by adsorption and persulfate oxidation in batch studies. *Industrial & Engineering Chemistry Research* **48**, 8373–8380.

Lin, K., Ding, J., Wang, H., Huang, X. & Gan, J. 2012 Goethite-mediated transformation of bisphenol A. *Chemosphere* **89**, 789–795.

Muhammad, S., Shukla, P. R., Tadé, M. O. & Wang, S. 2012 Heterogeneous activation of peroxymonosulphate by supported ruthenium catalysts for phenol degradation in water. *Journal of Hazardous Materials* **215–216**, 183–190.

Pang, Y., Ruan, Y., Feng, Y., Diao, Z., Shih, K., Hou, L. A., Chen, D. & Kong, L. 2019 Ultrasound assisted zero valent iron corrosion for peroxymonosulfate activation for Rhodamine-B degradation. *Chemosphere* **228**, 412–417.

Peng, G., Li, T., Ai, B., Yang, S., Fu, J., He, Q., Yu, G. & Deng, S. 2019 Highly efficient removal of enrofloxacin by magnetic montmorillonite via adsorption and persulfate oxidation. *Chemical Engineering Journal* **360**, 1119–1127.

Qiao, D., Li, Z., Duan, J. & He, X. 2020 Adsorption and photocatalytic degradation mechanism of magnetic graphene oxide/ZnO nanocomposites for tetracycline contaminants. *Chemical Engineering Journal* **400**, 125952–125963.

Rastogi, A., Al-Abed, S. R. & Dionysiou, D. D. 2009 Sulfate radical-based ferrous–peroxymonosulfate oxidative system for PCBs degradation in aqueous and sediment systems. *Applied Catalysis B: Environmental* **85**, 171–179.

Tang, L., Yu, J., Pang, Y., Zeng, G., Deng, Y., Wang, J., Ren, X., Ye, S., Peng, B. & Feng, H. 2018 Sustainable efficient adsorbent: Alkali-acid modified magnetic biochar derived from sewage sludge for aqueous organic contaminant removal. *Chemical Engineering Journal* **336**, 160–169.

Urase, T. & Kikuta, T. 2005 Separate estimation of adsorption and degradation of pharmaceutical substances and estrogens in the activated sludge process. *Water Research* **39**, 1289–1300.

Wang, X., Qin, Y., Zhu, L. & Tang, H. 2015 Nitrogen-doped reduced graphene oxide as a bifunctional material for removing bisphenols: synergistic effect between adsorption and catalysis. *Environmental Science & Technology* **49**, 6855–6864.

Wang, J., Liao, Z., Ifthikar, J., Shi, L., Du, Y., Zhu, J., Xi, S., Chen, Z. & Chen, Z. 2017 Treatment of refractory contaminants by sludge-derived biochar/persulfate system via both adsorption and advanced oxidation process. *Chemosphere* **185**, 754–763.

Wang, B., Li, Y.-N. & Wang, L. 2019 Metal-free activation of persulfates by corn stalk biochar for the degradation of antibiotic norfloxacin: activation factors and degradation mechanism. *Chemosphere* **237**, 124454–122463.

Xi, Y., Sun, Z., Hreid, T., Ayoko, G. A. & Frost, R. L. 2014 Bisphenol A degradation enhanced by air bubbles via advanced oxidation using in situ generated ferrous ions from nano zero-valent iron/palygorskite composite materials. *Chemical Engineering Journal* **247**, 66–74.

Xiao, P., Wang, P., Li, H., Li, Q., Shi, Y., Wu, X.-L., Lin, H., Chen, J. & Wang, X. 2018 New insights into bisphenols removal by nitrogen-rich nanocarbons: synergistic effect between adsorption and oxidative degradation. *Journal of Hazardous Materials* **345**, 123–130.

Yang, S., Yang, X., Shao, X., Niu, R. & Wang, L. 2011 Activated carbon catalyzed persulfate oxidation of Azo dye acid orange 7 at ambient temperature. *Journal of Hazardous Materials* **186**, 659–666.

Yang, L., He, L., Xue, J., Ma, Y., Xie, Z., Wu, L., Huang, M. & Zhang, Z. 2020 Persulfate-based degradation of perfluorooctanoic acid (PFOA) and perfluorooctane sulfonate (PFOS) in aqueous solution: review on influences, mechanisms and prospective. *Journal of Hazardous Materials* **393**, 122405–122415.

Yüksel, S., Kabay, N. & Yüksel, M. 2013 Removal of bisphenol A (BPA) from water by various nanofiltration (NF) and reverse osmosis (RO) membranes. *Journal of Hazardous Materials* **263**, 307–310.

Zhang, D., Pan, B., Zhang, H., Ning, P. & Xing, B. 2010 Contribution of different sulfamethoxazole species to their overall adsorption on functionalized carbon nanotubes. *Environmental Science & Technology* **44**, 3806–3811.

Zhang, B., Wu, T., Sun, D., Chen, W., Li, G. & Li, Y. 2019 NH2-MCM-41 supported on nitrogen-doped graphene as bifunctional composites for removing phenol compounds: synergistic effect between catalytic degradation and adsorption. *Carbon* **147**, 312–322.

Zhou, J., Ma, F. & Guo, H. 2020 Adsorption behavior of tetracycline from aqueous solution on ferroferric oxide nanoparticles assisted powdered activated carbon. *Chemical Engineering Journal* **384**, 123290–123297.

First received 7 September 2020; accepted in revised form 8 October 2020. Available online 6 November 2020